

**A peer-reviewed version of this preprint was published in PeerJ on 11 September 2019.**

[View the peer-reviewed version](https://peerj.com/articles/7622) (peerj.com/articles/7622), which is the preferred citable publication unless you specifically need to cite this preprint.

Liu W, Ni J, Shah FA, Ye K, Hu H, Wang Q, Wang D, Yao Y, Huang S, Hou J, Liu C, Wu L. 2019. Genome-wide identification, characterization and expression pattern analysis of APYRASE family members in response to abiotic and biotic stresses in wheat. PeerJ 7:e7622  
<https://doi.org/10.7717/peerj.7622>

# Genome-wide identification, phylogenetic and biochemical analysis of the APYRASE family members, and gene expression analysis in response to the abiotic and biotic stresses in bread wheat (*Triticum aestivum*)

Wenbo Liu<sup>Equal first author, 1, 2</sup>, Jun Ni<sup>Corresp., Equal first author, 2</sup>, Faheem Shah<sup>2</sup>, Kaiqin Ye<sup>3</sup>, Hao Hu<sup>2</sup>, Qiaojian Wang<sup>2</sup>, Dongdong Wang<sup>2</sup>, Yuanyuan Yao<sup>2</sup>, Shengwei Huang<sup>2</sup>, Jinyan Hou<sup>2</sup>, Chenghong Liu<sup>4</sup>, Lifang Wu<sup>Corresp. 2</sup>

<sup>1</sup> College of Life Sciences, University of Science and Technology of China, Hefei, China

<sup>2</sup> Key Laboratory of High Magnetic Field and Ion Beam Physical Biology, Hefei Institutes of Physical Science, Chinese Academy of Sciences, Hefei, China

<sup>3</sup> Anhui Province Key Laboratory of Medical Physics and Technology, Hefei Institutes of Physical Science, Chinese Academy of Sciences, Hefei, China

<sup>4</sup> Biotechnology Research Institute, Shanghai Academy of Agricultural Sciences, Shanghai, China

Corresponding Authors: Jun Ni, Lifang Wu

Email address: nijun@ipp.ac.cn, lfwu@ipp.ac.cn

APYRASEs, which directly regulated the intra- and extra-cellular ATP homeostasis, plays a pivotal role in the regulation of the adaptations to various stresses in mammals, bacteria and plants. In the present study, we identified and characterized the wheat APYRASE family members at the genomic level. The results showed that a total of eight APY homologs with conserved ACR domains were identified. The wheat APYs were further analyzed bioinformatically of their sequence alignment, phylogenetic relations and conserved motifs. Although they share highly conserved secondary structure and tertiary structure, the wheat APYs could be mainly categorized into three groups, according to the phylogenetic and structural analysis. Further, these APYs exhibited similar expression patterns in the root and shoot, among which *TaAPY3-1* and *TaAPY3-3* had the highest expression level. The time-course expression patterns of the eight APYs in the wheat seedlings in response to the biotic stress and abiotic stress were also investigated. *TaAPY3-2*, *TaAPY3-3*, and *TaAPY6* exhibited strong sensitivity to all kinds of stresses in the leaves. Some APYs showed specific expression responses, such as *TaAPY6* to the heavy metal stress, and *TaAPY7* to the heat and salt stress. These results suggested that the stress-inducible APYs could have potential roles in the regulation of the adaptation to the environmental stresses. Moreover, the catalytic activity of *TaAPY3-1* was further analyzed in the in vitro system. The results showed that *TaAPY3-1* protein exhibited high catalytic activity in degradation of ATP and ADP, but not GTP, CTP and TTP. It also has an extensive range of temperature adaptability, but rather preferred relative acid pH conditions. In this study, the genome-wide identification and characterization of the APYs in wheat could be

useful for further genetic modifications to generate high-stress tolerant wheat cultivars.

1 **Genome-wide identification, phylogenetic and biochemical analysis of**  
2 **the APYRASE family members, and gene expression analysis in**  
3 **response to the abiotic and biotic stresses in bread wheat (*Triticum***  
4 ***aestivum*)**

5  
6 Wenbo Liu<sup>1,2,†</sup>, Jun Ni<sup>2,†,\*</sup>, Faheem Afzal Shah<sup>2</sup>, Kaiqin Ye<sup>3</sup>, Hao Hu<sup>1,2</sup>, Qiaojian Wang<sup>2</sup>,  
7 Dongdong Wang<sup>2</sup>, Yuanyuan Yao<sup>2</sup>, Shengwei Huang<sup>2</sup>, Jinyan Hou<sup>2</sup>, Chenghong Liu<sup>4</sup>,  
8 and Lifang Wu<sup>2,\*</sup>

9  
10 <sup>1</sup>College of Life Sciences, University of Science and Technology of China, Hefei, Anhui,  
11 PR China

12 <sup>2</sup>Key Laboratory of High Magnetic Field and Ion Beam Physical Biology, Hefei Institutes  
13 of Physical Science, Chinese Academy of Sciences, Hefei, Anhui, PR China

14 <sup>3</sup>Anhui Province Key Laboratory of Medical Physics and Technology, Center of Medical  
15 Physics and Technology, Chinese Academy of Sciences, Hefei, Anhui, PR China.

16 <sup>4</sup>Biotechnology Research Institute, Shanghai Academy of Agricultural Sciences,  
17 Shanghai, PR China.

18  
19 \*Correspondence: Lifang Wu: [nijun@ipp.ac.cn](mailto:nijun@ipp.ac.cn) and [lfwu@ipp.ac.cn](mailto:lfwu@ipp.ac.cn); Tel: +86-551-6559-  
20 1413

21 †These authors contributed equally to this work.

22

23 **ABSTRACT**

24 *APYRASEs*, which directly regulated the intra- and extra-cellular ATP homeostasis,  
25 plays a pivotal role in the regulation of the adaptations to various stresses in mammals,  
26 bacteria and plants. In the present study, we identified and characterized the wheat  
27 *APYRASE* family members at the genomic level. The results showed that a total of eight  
28 *APY* homologs with conserved ACR domains were identified. The wheat *APYs* were  
29 further analyzed bioinformatically of their sequence alignment, phylogenetic relations  
30 and conserved motifs. Although they share highly conserved secondary structure and  
31 tertiary structure, the wheat *APYs* could be mainly categorized into three groups,  
32 according to the phylogenetic and structural analysis. Further, these *APYs* exhibited  
33 similar expression patterns in the root and shoot, among which *TaAPY3-1* and *TaAPY3-*  
34 *3* had the highest expression level. The time-course expression patterns of the eight  
35 *APYs* in the wheat seedlings in response to the biotic stress and abiotic stress were also  
36 investigated. *TaAPY3-2*, *TaAPY3-3*, and *TaAPY6* exhibited strong sensitivity to all kinds  
37 of stresses in the leaves. Some *APYs* showed specific expression responses, such as  
38 *TaAPY6* to the heavy metal stress, and *TaAPY7* to the heat and salt stress. These  
39 results suggested that the stress-inducible *APYs* could have potential roles in the  
40 regulation of the adaptation to the environmental stresses. Moreover, the catalytic  
41 activity of *TaAPY3-1* was further analyzed in the in vitro system. The results showed that  
42 *TaAPY3-1* protein exhibited high catalytic activity in degradation of ATP and ADP, but  
43 not GTP, CTP and TTP. It also has an extensive range of temperature adaptability, but  
44 rather preferred relative acid pH conditions. In this study, the genome-wide identification

45 and characterization of the APYs in wheat could be useful for further genetic  
46 modifications to generate high-stress tolerant wheat cultivars.

## 47 INTRODUCTION

48 The environmental stresses, such as salt, cold, drought and the pathogens would cause  
49 significant damage to the plant cells, which could lead to disturbed intra- and extra-  
50 cellular ATP homeostasis (Cao et al., **2014**). The cellular ATP level was tightly controlled  
51 by the GDA1-CD39 nucleoside phosphatases, which were widely existed in the plants,  
52 animals, fungi and bacteria (Matsumoto et al., **1984**; Tong et al., **1993**). The APYRASES  
53 (APYs), which were a class of nucleoside triphosphate diphosphohydrolases (NTPDases),  
54 played an important role in maintaining NTP homeostasis. APYs can be generally  
55 divided into ecto- and endo-APY, according to their subcellular locations (Matsumoto et  
56 al., **1984**; Tong et al., **1993**; Thomas et al., 1999; Dunkley et al., **2004**). Ecto-apyrases  
57 were localized on cell surface while endo-apyrase were usually on Golgi, endoplasmic  
58 reticulum (ER) and intracellular vesicles (Leal et al., **2005**). Some ecto-apyrases had  
59 membrane-spanning domains at their N- and C-terminal, and endo-apyrases usually has  
60 glycosylation on the amino acid, which was important for its correct protein folding,  
61 membrane targeting, cellular allocation and enzyme activity (Smith and Kirley, 1999;  
62 Murphy and Kirley, **2003**; Wu et al., **2005**; Knowles, **2011**). Different from ATPases using  
63  $Mg^{2+}$  as a co-factor, APYs can use variety of divalent, including  $Ca^{2+}$ ,  $Mg^{2+}$ ,  $Mn^{2+}$  and  
64  $Zn^{2+}$  (YangJ and Y, **2011**). The cellular ATP level not only plays a pivotal role for the  
65 energy supply, but also regulated various cellular processes related to the abiotic stress  
66 responses, including  $Na^+/H^+$  exchange, vacuolar  $Na^+$  distribution,  $K^+$  homeostasis,  
67 reactive oxygen (ROS) species regulation, and salt-responsive expression of  $K^+/Na^+$   
68 homeostasis and plasma membrane repair (Sun et al., **2012a**). Thus, the cellular  
69 ATP homeostasis regulated by the APYs was important for maintaining the normal cell  
70 function.

71 In plants, it had been reported that APYs participate in various processes, including  
72 growth regulation, and stress responses (Clark et al., **2014**). So far, seven APY  
73 members have been identified and functionally characterized in *Arabidopsis* (Tsan-Yu et  
74 al., 2015). AtAPY1 and AtAPY2, which were located at the Golgi, were involved in the  
75 regulation of many aspects of plant growth and development, such as pollen germination,  
76 root growth and stomata closure (Iris et al., **2003**; Jian et al., 2007; Tsan-Yu et al., 2015;  
77 Yang et al., **2015**). Although AtAPY1 and AtAPY2 were endo-APYs, the mutation of  
78 which could cause significant elevation of extracellular ATP (eATP) (Wu et al., **2007**; Hui  
79 et al., 2014), demonstrating that the intracellular located APYs could also regulate the  
80 eATP homeostasis. AtAPY6 and AtAPY7 also played pivotal roles in pollen development  
81 through the regulation of polysaccharides synthesis (Yang et al., 2013). Overexpression  
82 of PeAPY2 in *Arabidopsis* led to significant cleavage of the reactive oxygen species  
83 (ROS) (Sun et al., **2012a**), which would make it more tolerant to the abiotic stresses.  
84 Recently in some other species, it had been suggested that the APYs were directly  
85 involved in the regulation of biotic and abiotic stress resistance, such as drought and salt  
86 tolerance in *Populus euphratic* (Sun et al., **2012b**; Shurong et al., **2015**), pathogen  
87 resistance in pea and tobacco (Shiraishi and Tomonori, **2013**; Sharma et al., **2014**),  
88 water logging response in soybean (Alam et al., 2010). These results demonstrated that  
89 APY played an important role in the regulation of stress adaptation. Nevertheless, the

90 molecular mechanism still largely remained unclear.

91 Due to the novel functions of APY in the stress responses, the identification and  
92 functional characterization of the *APY* family genes in the crops, were important for the  
93 improvement of the stress tolerance via genetic modifications using *APYs* as the  
94 molecular targets. So far in wheat, there is still in lack of the *APY*-related studies. Here,  
95 we firstly identified the *APY* members in wheat in the genomic level. A comprehensive  
96 characterization and phylogeny of the *TaAPYs* using the bioinformatic and biochemical  
97 methods were further performed. Meanwhile, the time-course expression pattern of  
98 these *APYs* genes in response to various abiotic and biotic stresses was investigated.  
99 Additionally, the in vitro enzymatic analysis was also performed to further prove the *APY*  
100 enzymatic activities in degradation of the NTPs. Conclusively, these results provided  
101 valuable insights in the bioinformatic and functional characteristics of the *APY* gene  
102 family in wheat, which would further benefit the molecular breeding aiming at generating  
103 the stress-tolerant wheat cultivars.

## 104 **Materials and methods**

### 105 **Screening of gene sequences**

106 The amino acid sequence of the seven *Arabidopsis thaliana* *APYs*, obtained from TAIR  
107 (<https://www.arabidopsis.org/>), were used to blast against the wheat transcriptome and  
108 genome databases (Appels et al., 2018). The *APY* candidates were accepted only if the  
109 protein contains the conserved Apyrase Conserved Region (ACR) (Steinebrunner et al.,  
110 2000).

### 111 **Phylogenetic analyses of APYs**

112 The protein sequences of *APYs* from other species were obtained from the NCBI  
113 database. The phylogenetic analysis was carried out using the MEGA5 with maximum  
114 likelihood method with 1000 bootstrap replicates and other parameters were set as  
115 default (Jones et al., 1992; Tamura et al., 2011).

### 116 **Structure analysis of TaAPYs gene and amino acid sequences**

117 The DNAMAN software was used to analyze the conservation property of CDS and  
118 amino acid (AA) sequences. The secondary structures of these proteins were predicted  
119 using the online tool NPS@SOPMA (<https://npsa-prabi.ibcp.fr/>). The structure analysis  
120 included percentage of each amino acid, position and number of alpha helix, Beta Bridge,  
121 Random coli, as showed in different colors. The motif analysis was carried out using the  
122 MEME motif analysis. The membrane spanning motif method was analyzed using the  
123 online tool TMHMM (Jianyi et al., 2013b; Jianyi et al., 2013a). The 3D models of tertiary  
124 structures were simulated using the Swiss-Model (<https://www.swissmodel.expasy.org/>)  
125 which is based on the automatic ExPASy (Expert Protein Analysis System) web server  
126 (Guex et al., 2010; Pascal et al., 2011 ; Waterhouse et al., 2016; Bertoni et al., 2017;  
127 Waterhouse et al., 2018).

### 128 **Abiotic and biotic stress treatment.**

129 Two-week-old wheat seedlings (Yangmai 158) were used for the stress treatment. 300



130 mM NaCl, 42°C, 200 mM CdCl<sub>2</sub>, and 300 mM mannitol were separately used as salt,  
131 heat, heavy metal and drought treatment as previously described (Ni et al., 2018). The  
132 wheat leaf and root were collected at 1, 3, 6, 12 and 24 h post treatment. The *Bgt* spores  
133 were inoculated on the wheat leaves as previously described. The leaf sample was taken  
134 at 24, 48, 72 and 96 h post inoculation. The samples were immediately frozen in the  
135 liquid nitrogen and stored at -80°C. Each sample was prepared with three biological  
136 replicates.

### 137 RNA isolation and quantitative real-time PCR

138 The Plant RNA kit (Omega, Shanghai, China) and TransScript one-step gDNA Removal  
139 and cDNA synthesis SuperMix (Transgen, Beijing, China) were separately used for RNA  
140 and cDNA synthesis. The qPCR was carried out using the SYBR Green PCR Kit (Qiagen,  
141 China) on the Lightcycler96 system (Roche, Swiss). Raw data were calculated using the  
142 software given in the Lightcycler96 system. The primer information was listed in the  
143 Table S3.

### 144 Vector construction, recombinant protein expression and protein purification

145 The CDS of *TaAPY3-1* with removed region of the membrane spanning domain, was  
146 cloned into the pET22a vector. The expression vector was then transformed into the  
147 *Escherichia coli* BL21. The transformed cells were cultured in the Luria-Bertani (LB)  
148 broth at 4°C till the OD600 reaches 0.8, and then induced with 0.5 mM isopropyl beta-D-  
149 1-thiogalactopyranoside (IPTG). The induced cells were cultured at 37°C for 5 hours. The  
150 cells were then harvested by centrifugation at 10000×g and resuspended with 20 ml lysis  
151 buffer (20 mM Tris, 500 mM NaCl, pH 7.6). The cells were then lysed by sonication as  
152 previously described (Ye et al., 2015).

153 The recombinant protein was further isolated from the denatured inclusion body by  
154 using the Inclusion Body Protein Extraction Kit (Shengong, Shanghai, China). Briefly, the  
155 denatured protein was renatured by urea gradient dialysis in 500 ml renaturing buffers  
156 (10 mM Tris-HCl, 100 mM NaCl, 2 mM reduced glutathione, 0.2 mM oxidized glutathione,  
157 pH 8.5). The concentrations of urea in the renaturing buffers were 6.0, 4.0, 2.0, 1.0, and  
158 0 M, respectively. Every dialysis step was carried out at 4°C for 12 h. After the refolding  
159 process, the insoluble protein was removed by centrifugation at 10,000×g for 30 min at  
160 4°C. The amount and purity of recombinant protein were assessed by using the BCA  
161 Protein Assay Kit (Shengong, Shanghai, China).

### 162 Protein catalytic activity assay

163 The reaction system was set as: 50 mM Tris-HCl, 8 mM CaCl<sub>2</sub>, 0.25 ng/ul BSA, 2.5 mM  
164 DTT, 150 mM NaCl, and 0.05% Tween 20 (100 ul) as previously described (Dong et al.,  
165 2012). Then, 10 mM ATP (or ADP, TTP, CTP and GTP) and 4 ug purified recombinant  
166 APY was added into this system. The catalytic activity was analyzed under different  
167 conditions (Temperature, pH, substrates, and ions) by using the Phosphate Assay Kit  
168 (Jiancheng, Nanjing, China).

## 169 Results

### 170 Genome-wide identification and phylogenetic analysis of the APY family members

## 171 in wheat

172 The protein sequences of the seven *Arabidopsis* APYs and the conserved ACR domains  
173 were used as the query sequences to BLAST against the recently published wheat  
174 genome and transcriptome database (Appels et al., **2018**). After careful validation of the  
175 candidates, a total of 24 APY members were identified with top hits for the AtAPY  
176 homologs (AtAPY1-7) in the wheat genome. These wheat APY candidates exhibited  
177 high sequence similarity and all contained five Apyrase Conserved Region (ACR)  
178 domains (Figure S1). The twenty four wheat APYs were further divided into eight groups,  
179 each group with three homologs located at different genome sets (A, B and D) (Table 1).  
180 The CDS information of these APYs was listed as supplementary Table S1. Based on  
181 the sequence similarity to the *Arabidopsis* APY homologs, the identified wheat APYs  
182 were separately named as *TaAPY1*, *TaAPY2*, *TaAPY3-1*, *TaAPY3-2*, *TaAPY3-3*,  
183 *TaAPY5*, *TaAPY6* and *TaAPY7*. As show in Table 1, the APY genes were predicted to  
184 encode 430 to 706 amino acids in length, with putative molecular weights ranging from  
185 46.446 to 77.557 kD, and the protein isoelectric points (PIs) from 5.93 to 9.2 (Table. 1).  
186 As the three copies of the APYs in different wheat genome set (A, B and D) had very  
187 high CDS sequence similarity (Table 1), thus the APYs from the genome set A were  
188 used in the following bioinformatic and biochemical analysis.

189 To investigate the evolutionary relationships among the APYs, a phylogenetic tress  
190 was constructed using the APY homologs from *Arabidopsis thaliana*, *Zea mays*, *Oryza*  
191 *sativa*, *Aegilops tauschii*, *Phoenix dacylifera*, and some other species (Table S2). The  
192 APYs can be mainly divided into three distinct groups (I, II, and II). Specifically, *TaAPY1*,  
193 *TaAPY2*, *TaAPY3-1*, *TaAPY3-2* and *TaAPY3-3* in Group I, *TaAPY5* and *TaAPY6* were  
194 clustered in Group II, and *TaAPY7* in Group III (Figure 1).

## 195 Gene structure and conserved motif analysis of the APY genes in wheat.

196 To investigate the structural diversity of the APYs, the online structural analysis tool NPS  
197 @ SOPMA (Deléage, **2017**) was used for conserved motif analysis. As showed in Figure  
198 2, the amino acid sequences of those eight APYs were highly conserved. Additionally, a  
199 total of 16 motifs can be detected among the APYs (Figure S2). Generally, the eight  
200 APYs all contained motif 1, 3, 5 and 8 (Figure 2). APYs in the same group had specific  
201 motifs, such as motif 12 to *TaAPY5* and 6 (Group II), motif 8 to *TaAPY3-1* and 3-3  
202 (Group I), motif 15 to *TaAPY1* and 2 (Group I), and motif 6 to *TaAPY 1, 2, 3-1, 3-2* and 3-  
203 3 (Group I) (Figure 2). Further, the membrane spanning motif (MSM) analysis showed  
204 that all the Group I APYs (*TaAPY1, 2, 3-1, 3-2* and 3-3) were predicted to contain only  
205 one MSM at N-terminal, whereas Group II APYs (*TaAPY5* and 6) had two MSMs,  
206 separately located at N- and C- terminal (Figure 3). Interestingly, it was predicted that the  
207 Group III APY (*TaAPY7*) contained three MSMs (Figure 3). As comparison, the MSM of  
208 the seven APY members from *Arabidopsis* were also analyzed. The results showed that  
209 except *AtAPY5* and 7, which separately had two and three MSMs, the others only  
210 exhibited one MSM at the N-terminal, which was similar to the wheat APYs (Figure S3).  
211 The membrane-spanning was closely related to the protein allocation and transportation.  
212 Thus these results provided important information of their potential cellular roles.  
213 Moreover, the 3D structure analysis of the eight proteins showed that *TaAPY5, 6* and 7  
214 contains four subunits while other APYs only have two. Two similar subunits of the APY  
215 was linked with extended strand surrounded by alpha helix (Figure 4), which was a



216 signature character of GDA1-CD39 nucleoside phosphatase super family. Based on the  
217 results of 3D protein structure simulation (Figure 4), the eight wheat APYs can be also  
218 divided into two groups, Group I (TaAPY1, 2, 3-1, 3-2 and 3-3), and Group II (TaAPY5, 6  
219 and 7). Although TaAPY7 and TaAPY5, 6 were categorized into different groups in the  
220 phylogenetic tree, they shared high 3D structure similarity (Figure 1).

## 221 **Gene expression pattern of the APYs in response to the abiotic and abiotic** 222 **stresses in the wheat seedlings**

223 To investigate the expression pattern of the eight APYs in the wheat, the gene  
224 expression in shoot and root, and their responses to the abiotic stresses (salt, heat,  
225 heavy metal and osmotic stresses), were further analyzed by the quantitative real-time  
226 PCR. The results showed that all the eight APYs had similar expression level at the  
227 seedling shoot and root, with the highest expression level of *TaAPY3-1* and *TaAPY3-3*,  
228 and the lowest level of *TaAPY6* both in the shoot and root (Figure 5), suggesting  
229 *TaAPY3-1* and *TaAPY3-3* could be the predominant APYs in wheat.

230 Previous studies had shown that several APYs could be involved in the regulation of  
231 the abiotic stress adaptation (Clark et al., 2014). Thus we further investigated the time-  
232 course expression profile of APYs in the leaf and root of the wheat seedlings in response  
233 to different abiotic stresses. The results showed that in the leaves, most of the APYs  
234 could be upregulated after subjected to the cadmium treatment (Figure 6A). Specifically,  
235 the expression of *TaAPY3-1* reached a peak at 6 h in the leaves. The expression of the  
236 other APYs in the root was not as sensitive as that in the stem, only *TaAPY6* exhibited a  
237 significant upregulation at 6 h (Figure 6A). Further, mannitol treatment was used to  
238 produce an artificial drought stress condition in the wheat seedlings. The results showed  
239 that, all the APYs could be up-regulated within 24 h, among which, *TaAPY1* and *TaAPY6*  
240 reached an extremely high expression level in the leaves (Figure 6B). As contrary, very  
241 few genes exhibited significant changes at different time post mannitol treatment in the  
242 root (Figure 6B), suggesting these APYs regulated the drought responses in the shoot,  
243 but only in the root. Under heat stress, not until at 12 h, the expression of *TaAPY7*,  
244 *TaAPY6*, *TaAPY5* and *TaAPY3-2* began to increase both in the leaves and root, with the  
245 highest increase fold of *TaAPY3-2* (Figure 6C). For salt stress, the expression of all the  
246 *TaAPYs* was significantly increased in the leaves at 12 h, whereas in the root, only  
247 *TaAPY1*, *TaAPY7*, and *TaAPY5* were shortly up-regulated, while others remained  
248 unaffected all the time (Figure 6D).

249 As for biotic stress, powdery mildew pathogen was used to stress the wheat  
250 seedlings. The results showed that seven APYs (except *TaAPY1*) showed significant  
251 sensitivity to *Blumeria graminis* infection. Specifically, the significant up-regulation of  
252 *TaAPY2*, *TaAPY3-1*, *TaAPY3-2*, *TaAPY5* and *TaAPY6* could be detected at the pre-  
253 penetration stage (24 h), whereas *TaAPY3-3* and *TaAPY7* were significantly up-  
254 regulated at the late infection stages (Figure 7). These results suggested that the wheat  
255 APYs could be involved in the regulation of biotic stress responses. Nevertheless,  
256 different APYs may have diverse roles at different infection stages.

## 257 **Enzymatic analysis of the recombinant APY3-1 in wheat**

258 To further validate the enzymatic activity of the wheat APYs, the recombinant APY3-1

259 without the cross-membrane domain was cloned and purified using the *Escherichia coli*  
260 expression system (Figure 8A and B). The production of the inorganic phosphate in the  
261 system was used to determine ATP hydrolyzation as previously described (Dong et al.,  
262 **2012**). The results showed that the recombinant TaAPY3-1 exhibited high enzymatic  
263 activity with a relatively wide range temperature from 25 to 52°C, and had the highest  
264 catalytic activity at 37°C (Figure 8C). Further, the APY3-1 had relatively high enzyme  
265 activities at the acid conditions, with maximal activity detected at pH 4.5 to 5.5 (Figure  
266 8D). Moreover, the hydrolyzation efficiency of APY3-1 on different substrates was also  
267 evaluated. The results showed that the APY3-1 exhibited slightly lower enzymatic activity  
268 on degrading the ADP compared with ATP, while had very lower activity on the  
269 degradation of TTP, GTP and CTP, suggesting that the TaAPY3-1 had high substrate  
270 preference (Figure 8E). Moreover, it has been demonstrated that all the NTPDase family  
271 members require divergent metal ions as cofactors for their enzymatic activity. Thus, we  
272 also evaluated different ions on the enzymatic activity in degrading the ATP. The results  
273 showed that Ca<sup>2+</sup> was proved to be the most effective cofactor than others. The  
274 preference order was as follows: Ca<sup>2+</sup> > Mg<sup>2+</sup> > Zn<sup>2+</sup> (Figure 8F). Without the ions, the  
275 APY3-1 completely lost the enzymatic activity, suggesting that the apyrase activity is  
276 dependent on the ions as cofactors, with the preference for Ca<sup>2+</sup>. The catalytic activity of  
277 TaAPY3-1 can reach a peak of V<sub>max</sub>=61 (Pi uM/h/ug protein), K<sub>m</sub>=8.7 mM under the  
278 most appropriate conditions (37°C, pH 5.5, 8 mM Ca<sup>2+</sup>) (Figure 8G). Conclusively, these  
279 results suggested that the APY3-1 had high and specific ATP and ADP degradation  
280 activities, which was consistent with the functions of the APY homologs reported in other  
281 species.

## 282 Discussion

283 The cellular ATP homeostasis not only played a pivotal role in maintaining normal cell  
284 growth and development, but was also important for the regulation of stress responses  
285 (Clark and Roux, 2018). APYASEs (APYs) played a key role in maintaining regular cell  
286 growth and stress responses, mainly by the regulation of the extra- and intra-cellular  
287 ATP level, and the Golgi-based glycoprotein synthesis (Kiwamu et al., 2010; Clark et al.,  
288 **2014**). Stresses could cause significant eATP efflux from the cell, which led to increased  
289 ROS accumulation and further induce cell apoptosis (Jeter et al., 2004; Song et al., 2006;  
290 Kiwamu et al., 2010; Vadim et al., 2010). Thus the efficient cleavage of the over-dosed  
291 eATP could be important for prevention of the stress-induced cell apoptosis. Recent  
292 researches showed that overexpression of the APY could significantly inhibit the ROS  
293 production and promote the stress resistance (Shurong et al., **2015**). Thus, the  
294 regulation of the endo- and extracellular ATP level manipulated by the APYs could be  
295 the potential target to improve the stress resistance. In this paper, we firstly identified  
296 and characterized the *TaAPY* family members at the genomic level. The results showed  
297 that a total of eight APY genes, which all contained the conserved ACR domains, were  
298 identified in the wheat genome (Table 1). The identification and characterization of the  
299 APYs could provide valuable insight into the physiological and biochemical functions of  
300 wheat APYs in the stress responses.

301 In wheat genome, a total of eight APY members were identified. Similar to the  
302 categorization of the AtAPY1-7 in *Arabidopsis* (Tsan-Yu et al., 2015), the identified  
303 wheat APYs can be also divided into three groups. It has been postulated that the

304 transmembrane character could be associated with the subcellular locations of the  
305 proteins. TaAPY5 and TaAPY6 contained both N- and C-membrane spanning motifs  
306 (MSMs), and TaAPY7 had three MSMs (Figure 3). It has been reported that all four ecto-  
307 APYs from the human contained both N- and C-terminal transmembrane domains,  
308 others which contained only C-terminal transmembrane domains were endo-APYs  
309 (Knowles, **2011**; Tsan-Yu et al., 2015). In *Arabidopsis*, although AtAPY6 and AtAPY7  
310 contained both N- and C-terminal MSM (Figure S3), it was localized to the ER, similar to  
311 the other AtAPYs (Tsan-Yu et al., 2015). These results suggested that the MSMs cannot  
312 be considered as the protein location marker as it did in the mammalian. Although APY1-  
313 7 in *Arabidopsis* were proved to be inter-cellular located, they could also affect the extra-  
314 cellular ATP level, which was important for the stress responses. It has been revealed  
315 that APY1 and APY2 mutation in *Arabidopsis*, could cause significant elevation of the  
316 eATP level (Wu et al., **2007**; Hui et al., 2014), suggesting the eATP homeostasis could  
317 also be regulated by the endo-APYs in plants.

318 The investigation of the gene expression pattern in response to the stresses could  
319 help to identify the gene function (Wang et al., 2018; Wang et al., 2019). In wheat, the  
320 correlation between the diversely regulated APY expression and the stresses, provided  
321 evidences that the APYs could be directly or indirectly involved in the regulation of the  
322 stress adaptation (Figure 6 and 7). The results showed that different APYs exhibited  
323 various expression patterns in response to different stresses, and even varied in different  
324 organs (Figure 5-7). Generally, the expression of most APYs (including TaAPY1,  
325 TaAPY2, TaAPY3-1, TaAPY3-3, TaAPY7 and TaAPY6) was up-regulated in the leaf  
326 under drought stress, and barely upregulated in root except TaAPY5 and TaAPY6  
327 (Figure 6). For salt stress, except TaAPY3-1, TaAPY3-2, and TaAPY3-3, other genes  
328 exhibited significant up-regulation in the root (Figure 6). Specifically, the significant up-  
329 regulation of 20 times can be detected in the wheat seedlings in response to various  
330 stress conditions, such as TaAPY1, TaAPY6 to drought stress, TaAPY3-2, TaAPY6 and  
331 TaAPY7 to heat stress (Figure 7). Specifically, our results also showed that the  
332 expression of most APYs was biotic stress-responsive. The expression of TaAPY2,  
333 TaAPY3-1, and TaAPY5 exhibited significant up-regulation at 24 h after powdery mildew  
334 inoculation (Figure 7). As shown in figure 7, the powdery mildew spores started to  
335 colonize at the cell surface at 24 h. The transient up-regulation of these three APYs  
336 indicated that they were involved in the primary defense in the wheat leaves, after  
337 subjected to the powdery mildew. The expression of almost all the APYs was inhibited at  
338 48 to 72 hours, while increased at 96 h, when new *Bgt* spores were formed and started  
339 to infect the leaves again. Thus the expression pattern of these APYs indicated that the  
340 APYs could function at the pre-invasive stages in response to the biotic stresses.  
341 Conclusively, the wheat APYs were mostly stress-responsive, and some exhibited the  
342 stress specificity.

343 The recombinant protein of TaAPY3-1 was purified and its enzymatic activity was  
344 further evaluated under different conditions. Unlike the ecto-APY (NTPDase1) from  
345 human lymphocytes (Leal et al., **2005**), the TaAPY3-1 protein exhibited high stability  
346 within a much wider temperature range from 4°C to 60°C, and reached the highest activity  
347 at 37°C (Figure 8). Further, a relative alkaline conditions were required for the enzymatic  
348 activities of NTPDase1 (Leal et al., **2005**), while the appropriate reaction pH for TaAPY3-  
349 1 was only 4.5 to 5.5. The buffer pH over 7 in the reaction buffer almost diminished the

350 enzymatic activity of TaAPY3-1 (Figure 8). This could be due to the different subcellular  
351 locations of the APY members, where the pH of different cell compartment was different.  
352 Meanwhile, in *Arabidopsis*, the AtAPY3 showed relative high enzymatic activity in  
353 hydrolyzing the ATP, UTP, GTP and CTP, and also can hydrolyze ADP and GDP (Tsan-  
354 Yu et al., 2015). Although TaAPY3-1 and AtAPY3 were homologous proteins, the  
355 TaAPY3-1 only exhibited high enzymatic activity to ATP and ADP, low activity to TTP  
356 and GTP, and no activity to CTP. These results demonstrated that the homologs in  
357 different species, might function differently, and TaAPY3-1 in wheat was an ATP/ADP-  
358 specific APY.

## 359 CONCLUSION

360 In this study, we identified and characterized the APY family members in wheat at the  
361 genome-wide level. The phylogenetic, structural and expression analysis provided a  
362 theoretical basis for further functional study and the genetic improvement during the  
363 molecular breeding for generation of the stress-resistant wheat cultivars.

## 364 ACKNOWLEDGEMENTS

365 We thank the lab colleagues for critically reading the manuscript.

## 366 References

- 367 Alam, I., Lee, D.G., Kim, K.H., Park, C.H., Sharmin, S.A., Lee, H., Oh, K.W., Yun, B.W.  
368 and Lee, B.H., 2010. Proteome analysis of soybean roots under waterlogging  
369 stress at an early vegetative stage. *J.J.o.B.* 35, 49-62.
- 370 Appels, R., Eversole, K., Feuillet, C., Keller, B., Rogers, J., et al., 2018. Shifting the limits  
371 in wheat research and breeding using a fully annotated reference genome.  
372 *Science* 361, 661-+.
- 373 Bertoni, M., Kiefer, F., Biasini, M., Bordoli, L. and Schwede, T., 2017. Modeling protein  
374 quaternary structure of homo- and hetero-oligomers beyond binary interactions by  
375 homology. *Sci. Rep.* 7, 10480.
- 376 Cao, Y., Tanaka, K., Nguyen, C.T. and Stacey, G., 2014. Extracellular ATP is a central  
377 signaling molecule in plant stress responses. *Curr. Opin. Plant Biol.* 20, 82-87.
- 378 Clark, G. and Roux, S.J., 2018. Role of Ca<sup>2+</sup> in Mediating Plant Responses to  
379 Extracellular ATP and ADP. *Int.J. Mol.Sci.* 19, 16.
- 380 Clark, G.B., Morgan, R.O., Fernandez, M.P., Salmi, M.L. and Roux, S.J., 2014.  
381 Breakthroughs spotlighting roles for extracellular nucleotides and apyrases in  
382 stress responses and growth and development. *Plant Sci.* 225, 107-16.
- 383 Deléage, G., 2017. ALIGNSEC: viewing protein secondary structure predictions within  
384 large multiple sequence alignments. *Bioinformatics* 33.
- 385 Dong, F., Fu, Y., Li, X., Jiang, J., Sun, J. and Cheng, X., 2012. Cloning, expression, and  
386 characterization of salivary apyrase from *Aedes albopictus*. *Parasitol. Res.* 110,  
387 931-937.
- 388 Dunkley, T.P.J., Watson, R., Griffin, J.L., Dupree, P. and Lilley, K.S., 2004. Localization



- 389 of organelle proteins by isotope tagging (LOPIT). *Mol. Cell. Proteom.* 3, 1128-  
390 1134.
- 391 Guex, N., Peitsch, M.C. and Schwede, T., 2010. Automated comparative protein  
392 structure modeling with SWISS-MODEL and Swiss-PdbViewer: A historical  
393 perspective. *Electrophoresis* 30, S162-S173.
- 394 Hui, L.M., Jian, W., Jianchao, Y., Gallardo, I.F., Dugger, J.W., Webb, L.J., James, H.,  
395 Salmi, M.L., Jawon, S. and Greg, C., 2014. Apyrase suppression raises  
396 extracellular ATP levels and induces gene expression and cell wall changes  
397 characteristic of stress responses. *Plant Physiol.* 164, 2054-2067.
- 398 Iris, S., Jian, W., Yu, S., Ashley, C. and Roux, S.J., 2003. Disruption of apyrases inhibits  
399 pollen germination in Arabidopsis. *Plant Physiol.* 131, 1638-1647.
- 400 Jeter, C.R., Wenqiang, T., Elizabeth, H., Tim, B. and Roux, S.J., 2004. Evidence of a  
401 novel cell signaling role for extracellular adenosine triphosphates and  
402 diphosphates in Arabidopsis. *Plant Cell* 16, 2652-2664.
- 403 Jian, W., Iris, S., Yu, S., Timothy, B., Jonathan, T., David, A., Antonio, G., Francis, J.,  
404 Stuart, R. and Roux, S.J., 2007. Apyrases (nucleoside triphosphate-  
405 diphosphohydrolases) play a key role in growth control in Arabidopsis. *Plant*  
406 *Physiol.* 144, 961-975.
- 407 Jianyi, Y., Ambrish, R. and Yang, Z., 2013a. BioLiP: a semi-manually curated database  
408 for biologically relevant ligand-protein interactions. *Nucl. Acids Res.* 41, 1096-103.
- 409 Jianyi, Y., Ambrish, R. and Yang, Z., 2013b. Protein-ligand binding site recognition using  
410 complementary binding-specific substructure comparison and sequence profile  
411 alignment. *Bioinformatics* 29, 2588-2595.
- 412 Jones, D.T., Taylor, W.R. and Thornton, J.M., 1992. The rapid generation of mutation  
413 data matrices from protein sequences. *Comput. Appl. Biosci.* 8, 275-282.
- 414 Kiwamu, T., Simon, G., Jones, A.M. and Gary, S., 2010. Extracellular ATP signaling in  
415 plants. *Trends in Cell Biology* 20, 601-608.
- 416 Knowles, A.F., 2011. The GDA1\_CD39 superfamily: NTPDases with diverse functions.  
417 *Puriner. Signal.* 7, 21-45.
- 418 Leal, D.B.R., Streher, C.A., Neu, T.N., Bittencourt, F.P., Leal, C.A.M., Silva, J.E.P.D.,  
419 Morsch, V.M. and Schetinger, M.R., 2005. Characterization of NTPDase  
420 (NTPDase1; ecto-apyrase; ecto-diphosphohydrolase; CD39; EC 3.6.1.5) activity  
421 in human lymphocytes. *Biochim. Et Biophys. Acta. General Subjects* 1721, 9-15.
- 422 Matsumoto, H., Yamaya, T. and Tanigawa, M., 1984. Activation of ATPase activity in  
423 the chromatin fraction of Pea nuclei by calcium and calmodulin. *Plant Cell Physiol.*  
424 25, 191-195.
- 425 Murphy, D.M. and Kirley, T.L., 2003. Asparagine 81, an invariant glycosylation site near  
426 apyrase conserved region 1, is essential for full enzymatic activity of ecto-  
427 nucleoside triphosphate diphosphohydrolase 3. *Biophys. Arch. Biochem.* 413, 107-  
428 115.
- 429 Ni, J., Wang, Q., Shah, F.A., Liu, W., Wang, D., Huang, S., Fu, S. and Wu, L., 2018.

- 430 Exogenous melatonin confers cadmium tolerance by counterbalancing the  
431 hydrogen peroxide homeostasis in wheat seedlings. *Molecules* 23, 799.
- 432 Pascal, B., Marco, B. and Torsten, S., 2011 Toward the estimation of the absolute quality  
433 of individual protein structure models. *Bioinformatics* 27, 343-350.
- 434 Sharma, T., Morita, E.H. and Abe, S., 2014. Expression pattern of *PsAPY1* during apical  
435 hook development in pea. *Biologia* 69, 293-299.
- 436 Shiraishi and Tomonori, 2013. Suppression of defense response related to plant cell wall.  
437 *Japan Agri. Res.Quart.* 47, 21-27.
- 438 Shurong, D., Jian, S., Rui, Z., Mingquan, D., Yinan, Z., Yuanling, S., Wei, W., Yeqing, T.,  
439 Dandan, L. and Xujun, M., 2015. *Populus euphratica* Apyrase2 enhances cold  
440 tolerance by modulating vesicular trafficking and Extracellular ATP in Arabidopsis  
441 plants. *Plant Physiol.* 169, 530-48.
- 442 Smith, T.M. and Kirley, T.L., 1999. Glycosylation is essential for functional expression of  
443 a human brain ecto-apyrase. *Biochemistry* 38, 1509-16.
- 444 Song, C.J., Iris, S., Xuazhi, W., Stout, S.C. and Roux, S.J., 2006. Extracellular ATP  
445 induces the accumulation of superoxide via NADPH oxidases in Arabidopsis.  
446 *Plant Physiol.* 140, 1222-1232.
- 447 Steinebrunner, I., Jeter, C., Song, C. and Roux, S.J., 2000. Molecular and biochemical  
448 comparison of two different apyrases from *Arabidopsis thaliana*. *Plant Physiol.*  
449 *Biochem.* 38, 913-922.
- 450 Sun, J., Zhang, C., Zhang, X., Deng, S., Zhao, R., Shen, X. and Chen, S., 2012a.  
451 Extracellular ATP signaling and homeostasis in plant cells. *Plant Signal. Behavior*  
452 7, 566-569.
- 453 Sun, J., Zhang, X., Deng, S., Zhang, C., Wang, M., Ding, M., Zhao, R., Shen, X., Zhou,  
454 X., Lu, C. and Chen, S., 2012b. Extracellular ATP signaling is mediated by H<sub>2</sub>O<sub>2</sub>  
455 and cytosolic Ca<sup>2+</sup> in the salt response of *Populus euphratica* cells. *Plos One* 7,  
456 e53136.
- 457 Tamura, K., Peterson, D., Peterson, N., Stecher, G., Nei, M. and Kumar, S., 2011.  
458 MEGA5: Molecular evolutionary genetics analysis using maximum likelihood,  
459 evolutionary distance, and maximum parsimony methods. *Mol. Biol. Evol.* 28,  
460 2731-2739.
- 461 Thomas, C., Sun, Y., Naus, K., Lloyd, A. and Roux, S., 1999. Apyrase functions in plant  
462 phosphate nutrition and mobilizes phosphate from extracellular ATP. *Plant*  
463 *Physiol.* 119, 543-551.
- 464 Tong, C.G., Dauwalder, M., Clawson, G.A., Hatem, C.L. and Roux, S.J., 1993. The  
465 major nucleoside triphosphatase in pea (*Pisum sativum* L.) nuclei and in rat liver  
466 nuclei share common epitopes also present in nuclear lamins. *Plant Physiol.* 101,  
467 1005-11.
- 468 Tsan-Yu, C., Jeemeng, L., Bianca, M., Dominique, L., Roux, S.J. and Heazlewood, J.L.,  
469 2015. Biochemical characterization of Arabidopsis APYRASE family reveals their  
470 roles in regulating endomembrane NDP/NMP homeostasis. *Biochem. J.* 472, 43.



- 471 Vadim, D., Zhonglin, S., Ryoung, S., Elinor, T., Lourdes, R., Anuphon, L., Mortimer, J.C.,  
472 Stephen, C., Slabas, A.R. and Glover, B.J., 2010. Plant extracellular ATP  
473 signalling by plasma membrane NADPH oxidase and Ca<sup>2+</sup> channels. *Plant J.* 58,  
474 903-913.
- 475 Wang, G., Wang, T., Jia, Z.H., Xuan, J.P., Pan, D.L., Guo, Z.R. and Zhang, J.Y., 2018.  
476 Genome-Wide Bioinformatics Analysis of MAPK Gene Family in Kiwifruit  
477 (*Actinidia Chinensis*). *Int. J. Mol. Sci.* 19, 16.
- 478 Wang, Q., Ni, J., Shah, F., Liu, W., Wang, D., Yao, Y., Hu, H., Huang, S., Hou, J., Fu, S.  
479 and Wu, L., 2019. Overexpression of the Stress-Inducible SsMAX2 Promotes  
480 Drought and Salt Resistance via the Regulation of Redox Homeostasis in  
481 *Arabidopsis*. *Int. J. Mol. Sci.* 20.
- 482 Waterhouse, A., Bertoni, M., Bienert, S., Studer, G., Tauriello, G., Gumienny, R., Heer,  
483 F.T., De, T.B., Rempfer, C. and Bordoli, L., 2018. SWISS-MODEL: homology  
484 modelling of protein structures and complexes. *Nucl. Acids Res.* 46, W296-W303.
- 485 Waterhouse, A., Studer, G., Tauriello, G., Bordoli, L., Bienert, S., de Beer, Tjaart A.P.  
486 and Schwede, T., 2016. The SWISS-MODEL Repository—new features and  
487 functionality. *Nucl. Acids Res.* 45, D313-D319.
- 488 Wu, J., Steinebrunner, I., Sun, Y., Butterfield, T., Torres, J., Arnold, D., Gonzalez, A.,  
489 Jacob, F., Reichler, S. and Roux, S.J., 2007. Apyrases (nucleoside triphosphate-  
490 diphosphohydrolases) play a key role in growth control in *Arabidopsis*. *Plant*  
491 *Physiol.* 144, 961-975.
- 492 Wu, J.J., Choi, L.E. and Guido, G., 2005. N-linked oligosaccharides affect the enzymatic  
493 activity of CD39: diverse interactions between seven N-linked glycosylation sites.  
494 *Mol. Biol. Cell* 16, 1661-1672.
- 495 Yang, J., Wu, J., Romanovicz, D., Clark, G., Roux, S.J. and Biochemistry, 2013. Co-  
496 regulation of exine wall patterning, pollen fertility and anther dehiscence  
497 by *Arabidopsis* apyrases 6 and 7. *J.P.P.* 69, 62-73.
- 498 Yang, X., Wang, B., Farris, B., Clark, G. and Roux, S.J., 2015. Modulation of root  
499 skewing in *Arabidopsis* by apyrases and extracellular ATP. *Plant Cell Physiol.* 56,  
500 2197.
- 501 Yang J and Y, S., 2011. Functional analyses of *Arabidopsis* apyrases 3 through 7.  
502 *Arabidopsis*.
- 503 Ye, K., Zhang, X., Ni, J., Liao, S. and Tu, X., 2015. Identification of enzymes involved in  
504 SUMOylation in *Trypanosoma brucei*. *Sci. Rep.* 5, 10097.
- 505  
506  
507  
508

# Figure 1

Phylogenetic analysis of the putative APYs in wheat and other plant species.

The phylogenetic tree was created using the MEGA5 software with maximum Likelihood method.

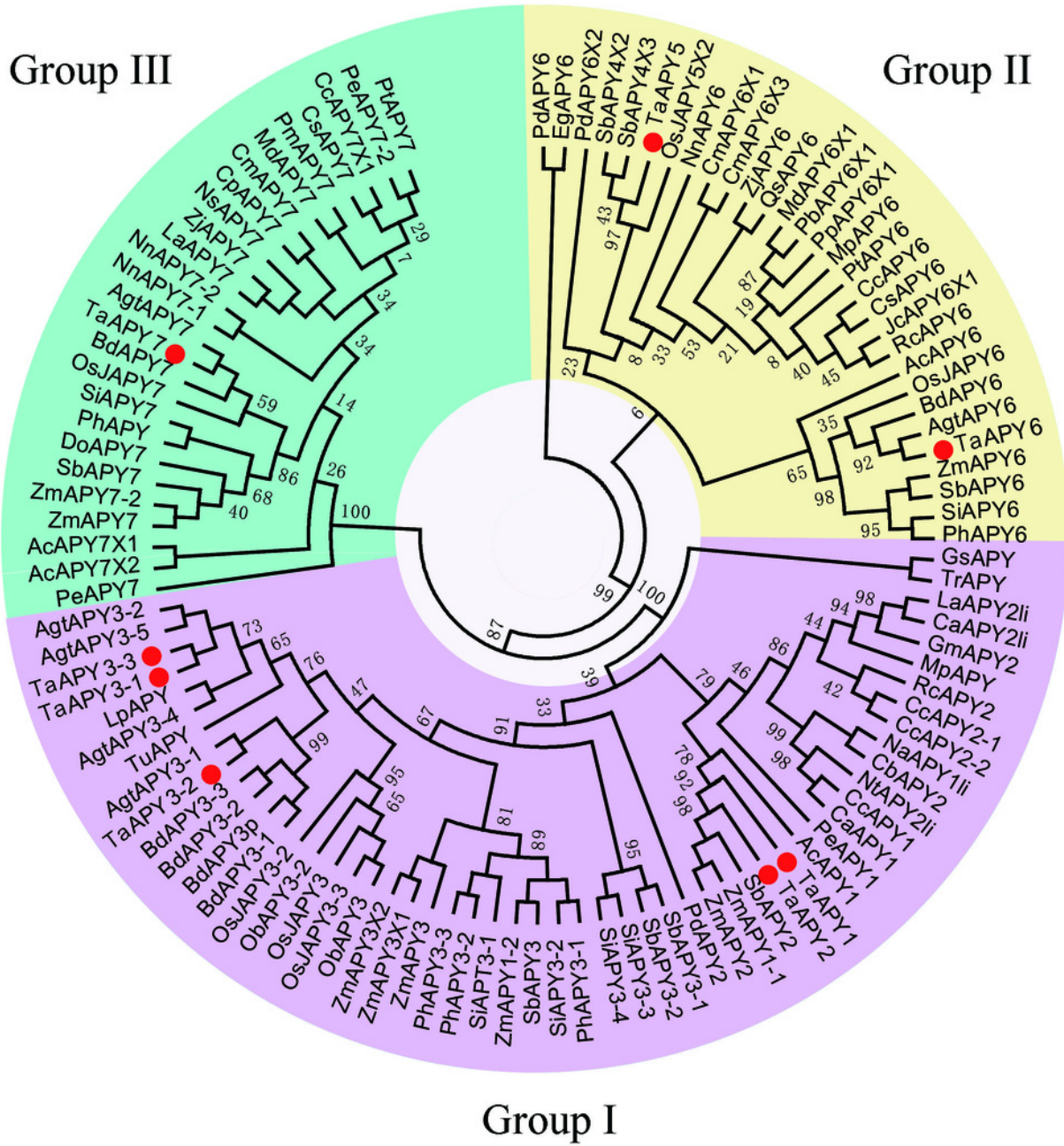


## Figure 2

Conserved motif analysis of the wheat APYs.

**(A)** The motif analysis of the eight APYs was carried out by using the online software MEME suite 5.0.2. **(B)** The details of the conserved motifs (1, 3, 5 and 8) of the eight APYs were represented, and other motifs were listed as supplementary material Figure S2. Different colors represent different motifs of the protein.

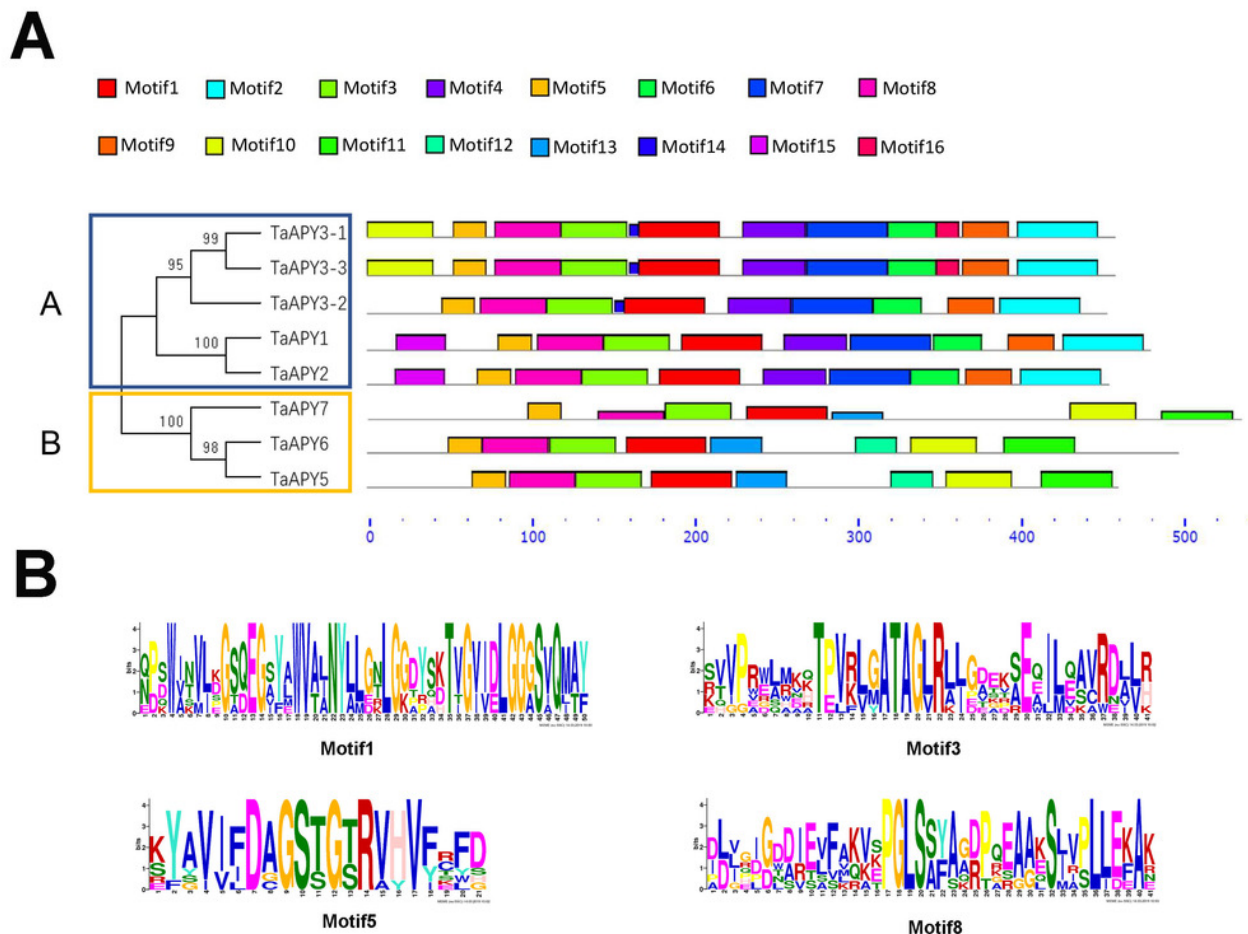




## Figure 3

Secondary structure analysis of the eight APYs.

Alpha helix was colored in red, Extend strand in blue and Random coil in purple. The cross membrane domain was predicted and marked with the red box.

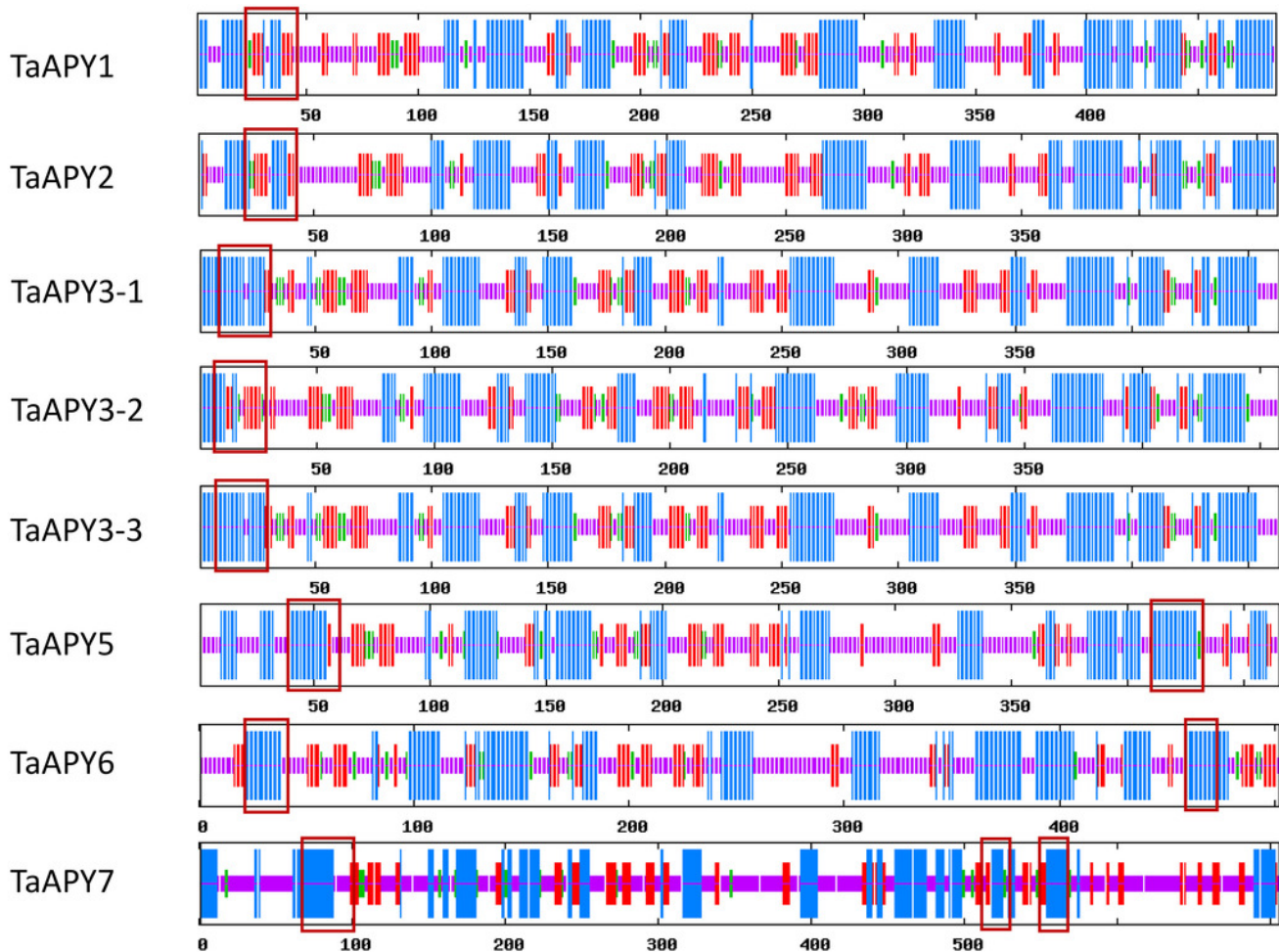
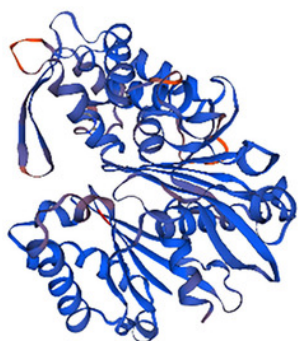


## Figure 4

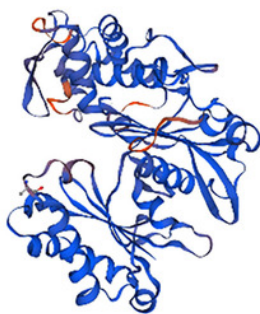
3D structure analysis of the eight wheat APYs.

Models were constructed using the Swiss-model website (

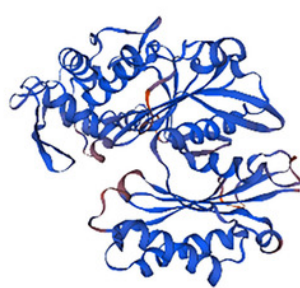
<https://www.swissmodel.expasy.org/> ).



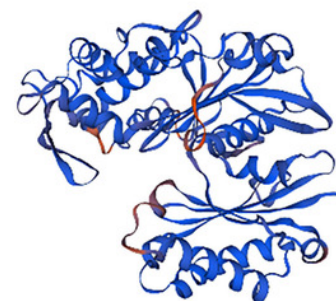
TaAPY1



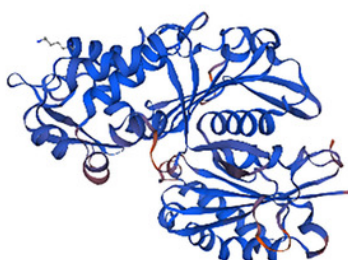
TaAPY2



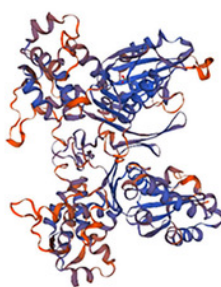
TaAPY3-1



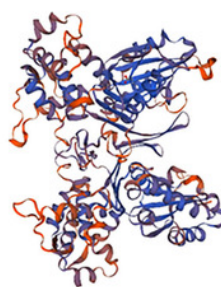
TaAPY3-2



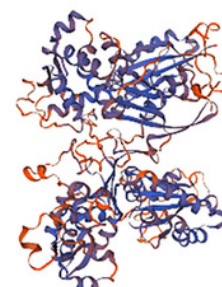
TaAPY3-3



TaAPY5



TaAPY6



TaAPY7



## Figure 5

Expression pattern of the eight *TaAPYs* in the root and leaf of the 10-d-old wheat seedlings.

*TaACT* was used as internal control. Data are presented as means  $\pm$  SD of three biological replicates.

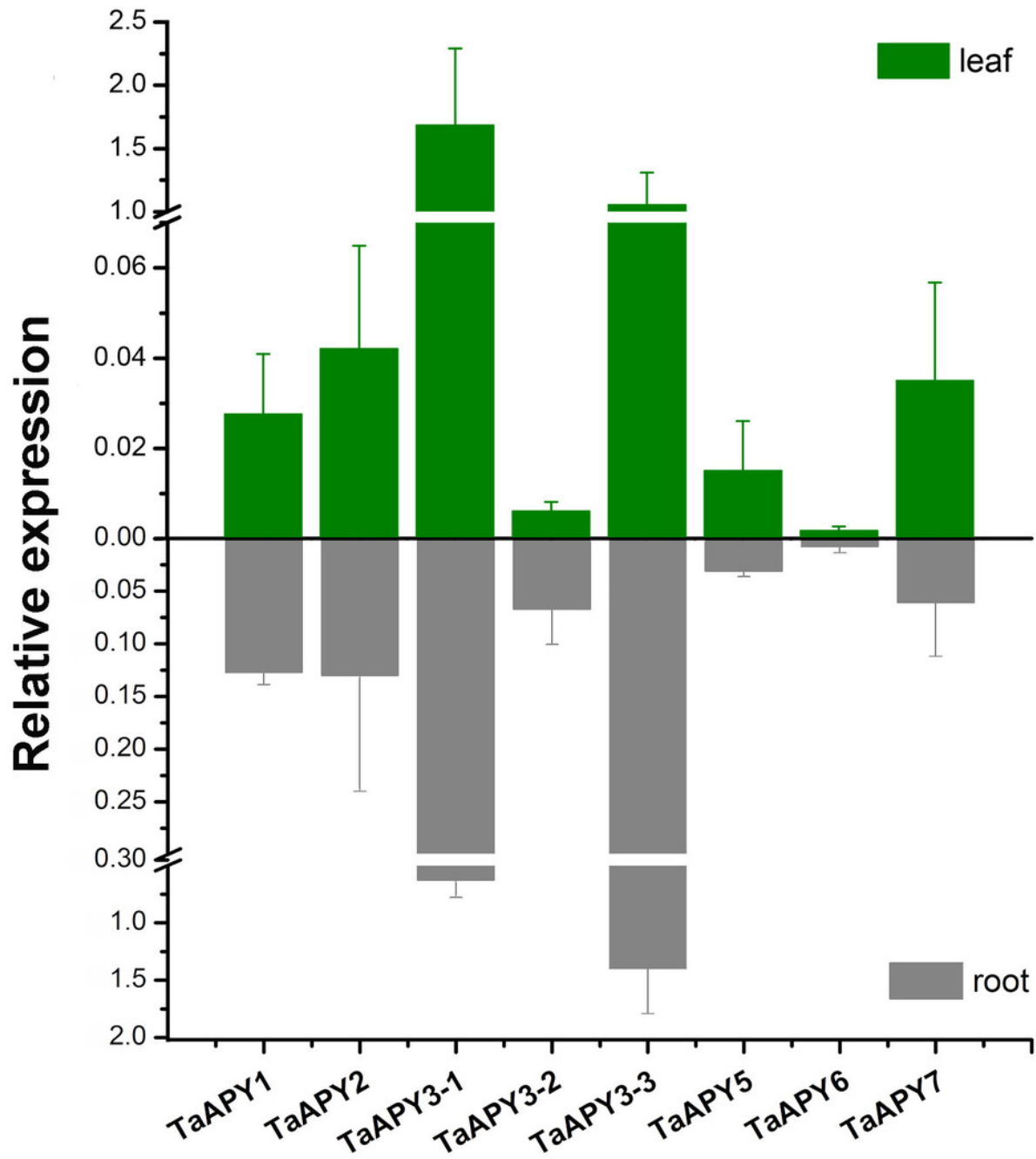


## Figure 6

Expression pattern of the wheat APYs in response to the abiotic stresses by qPCR.

**(A)** Heavy metal (200 mM CdCl<sub>2</sub>). **(B)** Drought (300 mM mannitol). **(C)** Heat (42°C). **(D)** Salt (300 mM NaCl). *TaACT* was used as internal control. Green and red colors represented decreased or increased expression level.

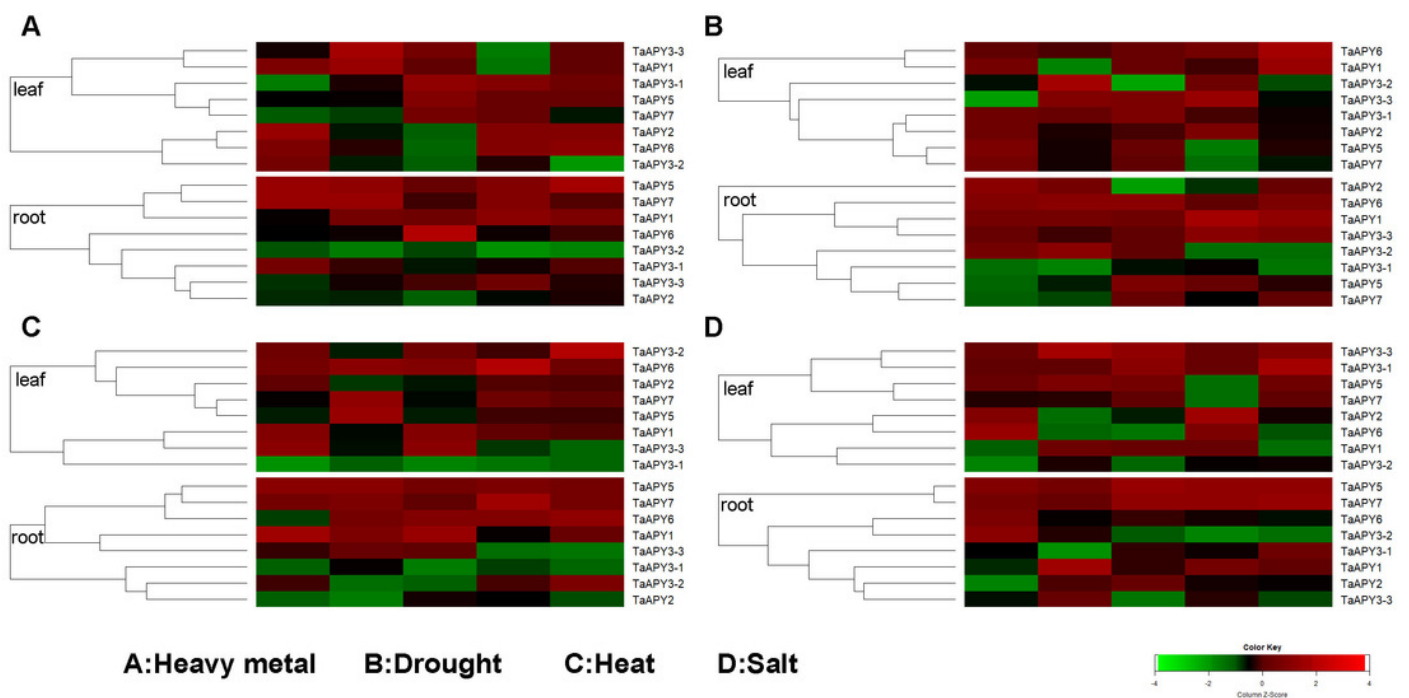


## Figure 7

Expression pattern of the *APYs* in response to the *Bgt* infection.

The expression of the *APYs* was analyzed separately at 24, 48, 72 and 96 h post *Bgt* infection. *TaACT* was used as the internal control. Green and red colors represented decreased or increased expression level.

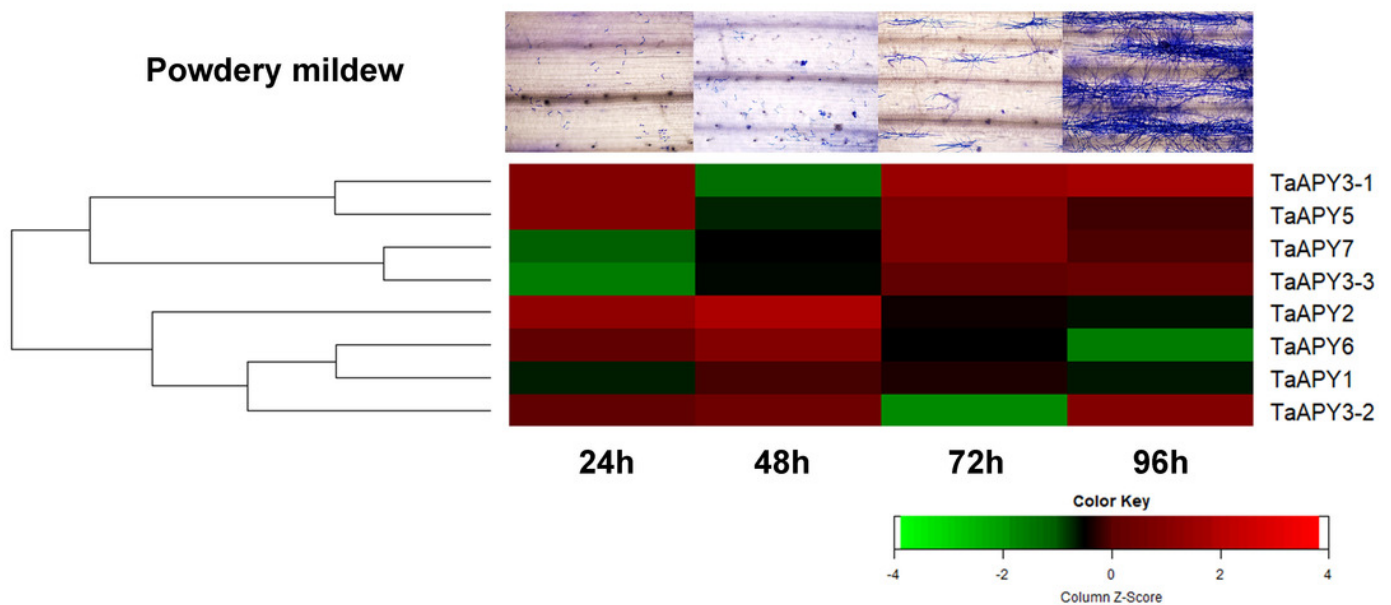


## Figure 8

Enzymatic activity analysis of recombinant TaAPY3-1.

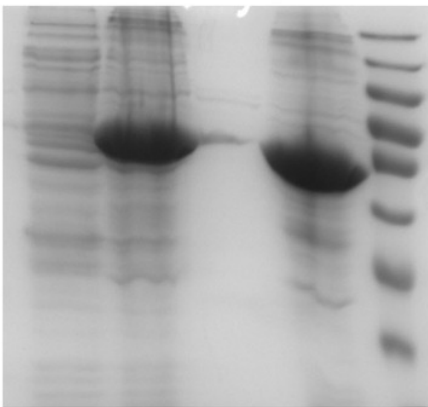
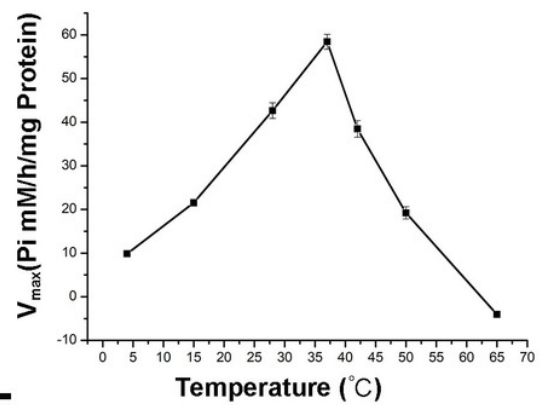
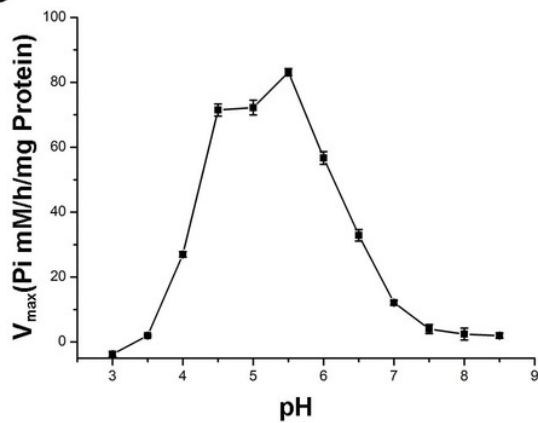
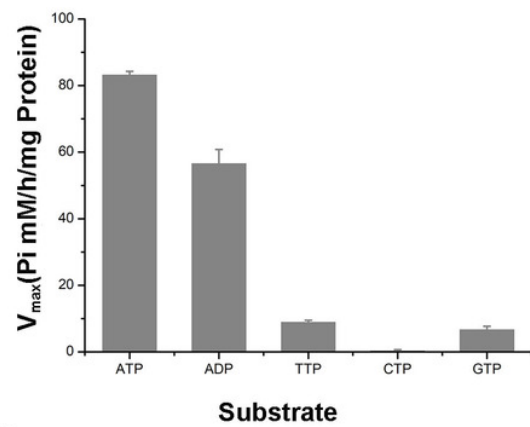
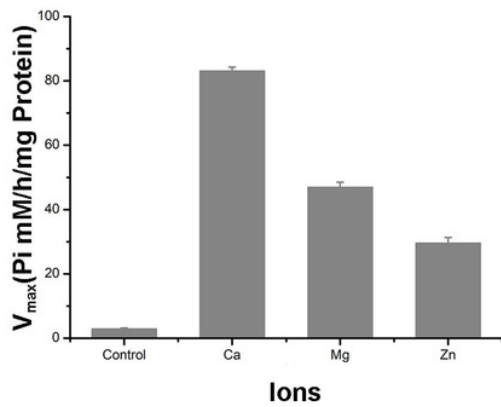
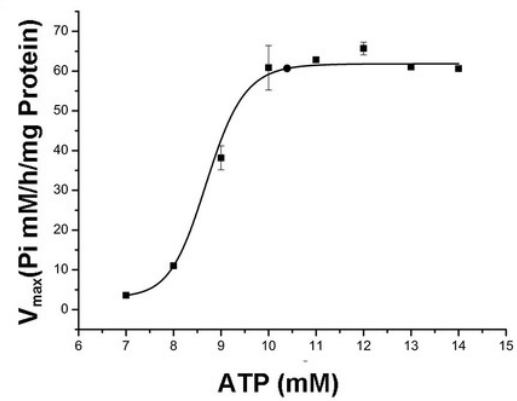
**(A)** Scheme of the purified TaAPY3-1 without the membrane spanning domain. **(B)** SDS-PAGE analysis of the protein purification. **(C)** Enzymatic activity of TaAPY3-1 in degradation of ATP under different temperature. **(D)** Activity of TaAPY3-1 under different pH. **(E)** Activity of TaAPY3-1 under different substrates. **(F)** Different ions on the enzymatic activity of TaAPY3-1. **(G)** Enzymatic activity analysis of TaAPY3-1 with different concentrations of ATP. Data are presented as means  $\pm$  SD of three biological replicates.

**A**

■ : Amino acid sequence

■ : Membrane spanning domain

■ : Apyrase activity site

**B****C****D****E****F****G**



**Table 1** (on next page)

Table 1. Characteristics of the APY members in wheat.

**Table 1.**  
**Characteristics of the**  
**APY**  
**members in**  
**wheat.**

CDS: coding sequence; AA: amino acid; MW: molecular weights; PI: protein isoelectric points.

Name	Gene ID	Protein length (AA)	CDS length (bp)	MW (kDa)	PI	Exon number	CDS similarity
TaAPY1	TraesCS4A01G131300.1	485	1458	52.225	5.93	10	
	TraesCS4B01G173300.1	485	1458	52.261	6.05	10	98
	TraesCS4D01G175400.1	485	1458	52.25	6.34	9	98
TaAPY2	TraesCS2A01G102100.1	457	1374	48.91	6.68	9	
	TraesCS2B01G119200.1	459	1380	49.08	6.68	9	97
	TraesCS2D01G101500.1	469	1410	50.034	7.04	9	98
TaAPY3-1	TraesCS5A01G532000.1	462	1389	49.471	6.05	7	
	TraesCS4B01G363700.1	462	1389	49.555	6.36	7	95
	TraesCS4D01G357100.1	463	1392	49.493	6.22	7	95
TaAPY3-2	TraesCS5A01G547700.1	457	1374	48.963	8.89	6	
	TraesCS4B01G381600.1	430	1293	46.446	8.81	6	94
	TraesCS4D01G357100.1	452	1359	49.036	6.06	10	83
TaAPY3-3	TraesCS7A01G160900.1	454	1365	49.196	5.96	7	
	TraesCS2B01G025000.1	449	1350	49.178	6.76	7	95
	TraesCS2D01G020200.2	448	1347	49.979	7.07	7	95
TaAPY5	TraesCS6A01G105900.1	502	1509	54.652	8.81	8	
	TraesCS7B01G178800.1	465	1398	51.287	8.96	8	96
	TraesCS7D01G280900.1	447	1344	49.209	8.02	6	96
TaAPY6	TraesCS6A01G105900.2	340	1023	36.015	8.13	8	
	TraesCS6B01G135200.1	502	1509	54.54	9.05	8	92
	TraesCS6D01G094400.2	502	1509	54.535	8.86	8	94
TaAPY7	TraesCS1A01G288900.1	706	2121	77.499	9.2	2	
	TraesCS1B01G298200.1	706	2121	77.557	9.19	2	98
	TraesCS1D01G287900.1	706	2121	77.472	9.2	2	98